This article has been accepted for publication in a future issue of this journal, but has not been fully edited. Content may change prior to final publication. Citation information: DOI 10.1109/TIM.2020.3016072, IEEE Transactions on Instrumentation and Measurement

Synchronous Detection to Reduce Offsets in Focus Error of an Optical Pickup Unit

Rekha S. Sekar, Arvind Ajoy

***Abstract*—The Optical Pickup Unit (OPU) is an optical assembly which is used for reading and writing digital optical disks. It consists of a laser diode, quadrant photodetector, and other optical components to maintain focus. This arrangement of the laser and photodetector is very similar to those in expensive equipment, such as atomic force microscopes, used for nanoscale metrology. Many researchers have hence investigated the use of an OPU to design low-cost alternatives. However, these non-standard uses of an OPU are challenging, since the OPU has originally been optimized to sense reflections from the highly reflecting surface of an optical disk. In this work, we present a new synchronous detection based method that improves the performance of the OPU in measuring the reflection from poorly reflecting substrates. This method utilizes the high bandwidth of both the laser and photodetector of the OPU. We excite the laser with a pulsed input, and look for a signal at the pulsing frequency in the output from the OPU. This signal is further processed through a phase-sensitive detector. We show that this method reduces the offsets in the measurement, and allows us to make effective use of a higher gain to measure the reflection from substrates with poor reflectivity.**

***Index Terms*—Optical Pickup Unit (OPU), synchronous detection, astigmatic focus detection, offsets**

I. Introduction

Digital Disks such as CDs, DVDs and Blu-ray disks store data as binary values. The data is either stored using physical variations of height on the disk's surface (pits and lands) or using variations of the reflective properties of different spots on the disk. The width of the data tracks on these discs decreases with increasing disk capacity, ranging from about 800 nm for a CD to 150 nm in a Blu-ray disk [1]. The data is read using an Optical Pickup Unit (OPU), which is a compact combination of optical components and associated electronics [2] that have been engineered to detect features down to approximately 100 nm. Modern OPUs, such as the PHR-803T (Toshiba Co., Tokyo, Japan) used inside the XBOX 360 (Microsoft Co., Redmond, USA), have three different laser diodes (with wavelengths 780nm, 650nm and 405nm) to read CDs, DVDs and Blu-ray disks using a single OPU. Further, owing to mass production, OPUs are available for a very low price (approximately USD 10 per piece). The OPU is hence a robust, compact, low-cost system that is capable of nanoscale measurements.

Many researchers have thus used commercially available OPUs as sensors in systems such as scanning probe microscopes [3], accelerometers [4], [5], [6], atomic force microscopes [7], vibrometers and bio-sensing systems [8], [9], [10]. OPUs have also been used for displacement sensing [11], [12], [13], alignment of substrates [14], and fabrication of masks [15]. These non-standard uses of an OPU can be challenging, since the OPU has originally been optimized to measure signals from the highly reflecting surface of an optical disk. Refer to Figure 1, which shows the impact of an offset in measurement. The outputs from the OPU are used to generate two quantities : (i) a Focus Error (S_{FE}) signal, and (ii) a Reflection signal R_F. Typically, S_{FE} is used in a control loop to maintain the objective lens of the OPU in focus with the target, in order to maximize R_F, as shown in Figure 1(a). A DC offset in S_{FE} causes the OPU to deviate from focus in the case of targets with high (Figure 1(b.i)) and

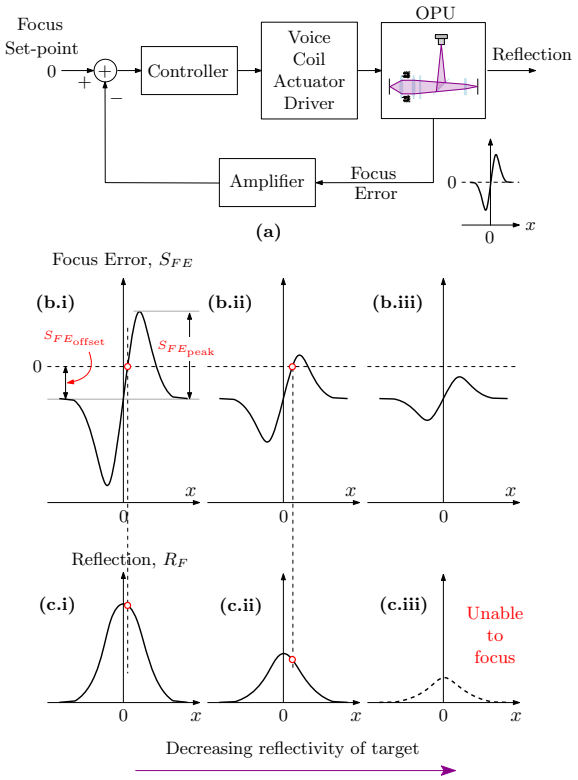

Fig. 1. (a) Typical focus control loop, wherein the controller drives a voice coil actuator to maintain the objective lens of the OPU in focus with the target. x depicts the deviation from focus, also called the 'Defocus distance'. The focus set-point of zero hence corresponds to $x = 0$. (b) Focus Error in the presence of a DC offset, for targets with (i) high reflectivity, (ii) medium reflectivity and (iii) poor reflectivity. (c) Corresponding reflection showing that offsets can cause the controller to lose focus when reflectivity is low.

Rekha S. Sekar and Arvind Ajoy are with Electrical Engineering, Indian Institute of Technology Palakkad, Palakkad, India. e-mail: 121703002@smail.iitpkd.ac.in, arvindajoy@iitpkd.ac.in

This article has been accepted for publication in a future issue of this journal, but has not been fully edited. Content may change prior to final publication. Citation information: DOI 10.1109/TIM.2020.3016072, IEEE Transactions on Instrumentation and Measurement

medium (Figure 1(b.ii)) reflectivity, leading to a deviation from measurement of peak reflection. Clearly, the deviation from peak reflection becomes more pronounced with decreasing target reflectivity. However, in the case of targets with poor reflectivity, S_{FE} can become entirely negative (or positive), causing the control loop to completely lose focus, making the measurement of R_F unreliable (Figure 1(b.iii, c.iii)). Further, it is not straightforward to compensate for the offset, since the offset can in general change with the gain of the OPU electronics.

In this work, we propose and demonstrate a method to significantly reduce the impact of offsets while using an OPU for nanoscale metrology. We make use of the fact that the photodetector, and the electronics in the OPU have a very high bandwidth ($>$ 100 MHz) [16] in order to read data from the spinning high-density optical disk. Additionally, we find that the laser diodes also have a large bandwidth of $\sim$ 20 kHz. Hence, we propose to pulse the laser diode (at a frequency $f_0 < 20$ kHz) and synchronously detect the component of the focus error and refection at the pulsing frequency, using a phase sensitive detector (PSD) followed by a low-pass filter. DC offsets from the OPU are eliminated. We show that this method can measure the focus error signal from a very dark, poorly reflecting surface – the standard DC measurement method applied to this sample results in a situation similar to Figure 1(b.iii, c.iii) wherein the amplitude of the focus error is swamped by the offset. To the best of our knowledge, this is the first report on synchronous detection by pulsing the laser diode of an OPU. We believe that our method can increase the dynamic range of reflectivities that an instrument made using an OPU can measure.

The paper is structured as follows. Section II reviews the construction of an OPU, and the origin of the focus error and reflection signals. Section III presents our implementation of the DC measurement method with constant illumination. Section IV describes our method for synchronous detection using a pulsed laser. Our results are presented and discussed in Section V. Finally, Section VI presents our conclusion.

II. Review

A. Optical Pickup Unit

A simplified schematic diagram of an OPU is shown in Figure. 2(a). The optical path is designed so that the light reflected by the target, when illuminated by any of the three laser diodes (405 nm, 650 nm and 780 nm), falls on a single photodetector. The polarizing beam splitter splits the light beam and makes it plane polarized. The quarter wave plate converts the plane polarized beam into a circularly polarized beam. Note that since the OPU has three lasers with three wavelengths, a single birefringent quarter wave plate cannot be used. Instead, a liquid crystal panel whose optical properties can be changed by application of a voltage, is used as a quarter wave plate in the OPU [17]. The collimating and movable objective lenses, along with the voice coil motor assembly, focuses the light on the target. Upon reflection, the light remains circularly polarized but with an opposite sense of polarization. This light, after returning through the quarter wave plate, becomes plane polarized with a polarization

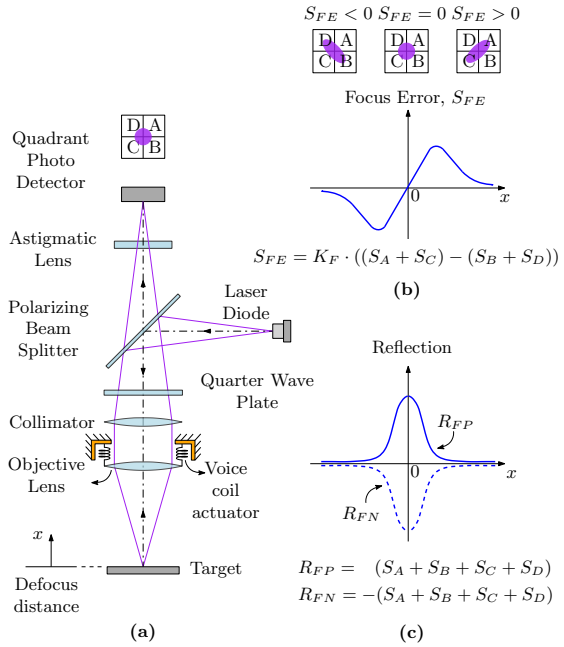

Fig. 2. (a) Typical construction of an Optical Pickup Unit. (b) Spot shape and Focus Error S_{FE} as the target is moved away from focus. S_X refers to the output from quadrant $X \in \{A, B, C, D\}$ of the photodetector and K_F is positive gain constant. (c) Reflection outputs R_{FP} and R_{FN} which can be used to generate the net reflection R_F from the target.

orthogonal to the initial polarization. This ensures that the incident and reflected rays do not interfere. The astigmatic lens and quadrant photodetector then provide a simple yet robust means [18], [19] of maintaining focus between the objective lens and substrate, as discussed in the next section. The OPU also has on-board electronics to control the laser diodes and voice coil actuator, and a Photodiode Integrated Circuit (PDIC) to measure the intensity of light falling on the photodiode array [16].

B. Focus Error and Reflection Signals

The astigmatic lens changes the shape of the laser beam falling on the photodetector, depending on deviation of the position of the target from the focal point of the objective lens [19], referred to as the 'Defocus distance', x. When the laser beam is perfectly focused on the target, the laser spot is circular and evenly spread on the four quadrants of the photo-detector (A, B, C, D), as shown in Figure 2(b). This corresponds to x = 0. When the target is slightly nearer to the objective lens than its focal length (i.e $x > 0$), the laser spot on the quadrant photodetector becomes an ellipse with its major axis along quadrants A, C. Similarly when $x < 0$, the laser spot is an ellipse along quadrants B, D. The focus error signal (S_{FE}) is generated by an external circuit as

$$S_{FE} = K_F \cdot ((S_A + S_C) - (S_B + S_D)) \tag{1}$$

where S_X is the output of quadrant X (X = A, B, C, D) provided by the OPU, and K_F is the gain provided by the external circuit. Hence, a zero focus error signal is developed if the target is at the focus of the objective lens (x = 0). Further, S_{FE} is proportional to x within a limited range of

This article has been accepted for publication in a future issue of this journal, but has not been fully edited. Content may change prior to final publication. Citation information: DOI 10.1109/TIM.2020.3016072, IEEE Transactions on Instrumentation and Measurement

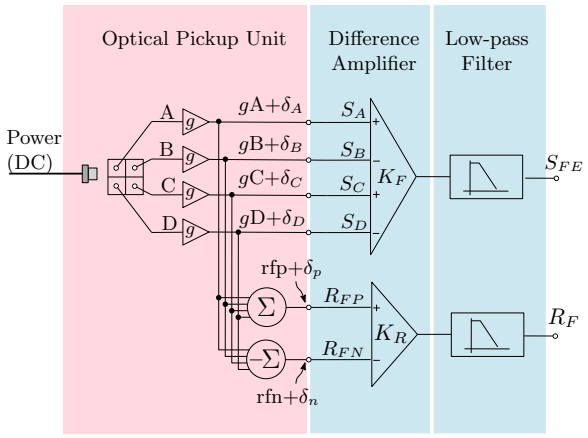

Fig. 3. Typical measurement method where the laser diode is powered by a constant DC supply. Note that all the outputs from the OPU: photodetector quadrants S_A, S_B, S_C, S_D and reflection R_{FP}, R_{FN} include offsets, denoted by δ. These offsets are a function of the internal gain g. The difference amplifiers and low-pass filters are external to the OPU.

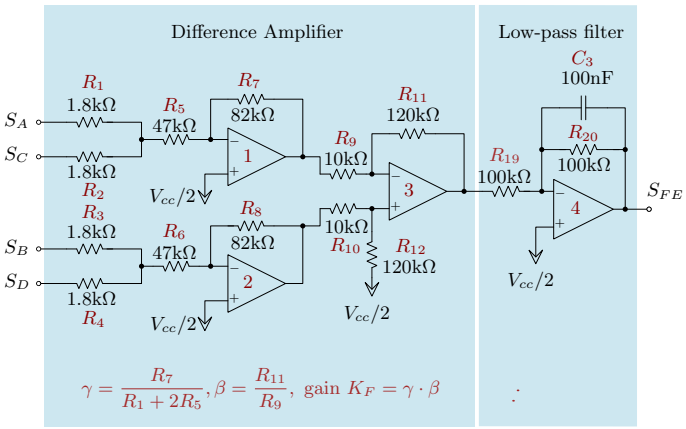

Fig. 4. Our implementation of a circuit to obtain S_{FE} from the outputs S_A, S_B, S_C, S_D of the OPU, as per the block diagram in Figure 3, with K_F = 10.3. Also, the low-pass filter, as implemented, provides an additional gain of -1. Note that the opamps have their positive terminals connected to $V_{cc}/2$, since the PHR-803T OPU references all outputs with respect to $V_{cc}/2$.

displacement. For large positive or negative values of x, the elliptical spot grows in size to cover all quadrants equally, thereby causing $S_{FE} \to 0$ again. The S_{FE} vs. x plot is often referred to as the 'S-curve' of the OPU [11]. It is used to control the voice coil actuator to maintain the target at the focus of the objective lens, using a control loop as discussed in Figure 1(a).

The OPU also provides positive and negative reflection signals R_{FP}, R_{FN} defined as

$$R_{FP} = (S_A + S_B + S_C + S_D) \quad (2a)$$

$$R_{FN} = -(S_A + S_B + S_C + S_D) \quad (2b)$$

These signals have to be combined externally to produce the net reflection

$$R_F = K_R \cdot (R_{FP} - R_{FN}) \quad (3)$$

from the target, where K_R is an external gain. Note that the magnitude of reflection is highest when the target is at the focal point of the objective lens (x = 0). Also, $R_F \to 0$ at large defocus distance, since the intensity of light falling on the photodetectors drops significantly for large defocus.

III. DC Measurement Technique

The typical measurement method powers the laser diode using a constant DC power supply [8], [11], [12]. Figure 3 shows the block diagram of a typical scheme used in this case, to generate S_{FE} and R_F from the outputs of the OPU. The PDIC inside the OPU uses transimpedance amplifiers to convert the current generated by the photodetectors into voltages. The gain g of these amplifiers can be set externally. In the PHR-803T, the gain g can be set to any of the following relative values: $2, 4, 8, 16, 32, 64, 128$. The difference amplifiers and low-pass filters are external to the OPU. The difference amplifiers generate the focus error and reflection signals based on eqs. (1, 3), while the low-pass filters remove high frequency noise.

All the outputs from the OPU have unintentional offsets. We denote these offsets as $\delta_A, \delta_B, \delta_C, \delta_D$ for the outputs of the four quadrants of the photodetector, and δ_p, δ_n for the positive, negative reflection signals. These offsets have two components: an electrical component, and an optical component. The *electrical offsets* arise from circuit elements inside the PDIC of the OPU, and are nominally specified to be within $\pm$25 mV for each of S_A, S_B, S_C, S_D and $\pm$40 mV for R_{FP}, R_{FN} in the PHR-803T [16]. In addition to the electrical offsets, there are internal reflections from the optical components of the OPU. We denote the component of measured signal due these internal reflections as the *optical offset*.

Figure 4 shows our implementation of the difference amplifier and low-pass filter for S_{FE}. The difference amplifier provides a K_F = 10.3. The low-pass filter provides an additional gain of -1. A similar circuit is used for R_F with K_R = 5.45. Note that the PHR-803T references all outputs S_A, S_B, S_C, S_D and R_{FN}, R_{FP} with respect to $V_{cc}/2$, where V_{cc} = 5V is the power supply voltage provided to the PDIC. This helps interfacing these outputs to a Digital-to-Analog converter in a DVD player. The positive terminals of the opamps in Figure 4 are hence connected to $V_{cc}/2$ to account for this level shift.

As discussed in Section II-B, both the focus error and reflection signals should approach zero for a large defocus distance. However, in practice, electrical and optical offsets cause a shift of these signals from zero. The net offsets in focus error and reflection will also include offsets from the opamps used in the external circuit, apart from the offsets generated by the OPU itself. R_F will have both electrical and optical offsets. On the other hand, S_{FE} will only have electrical offsets, since the optical offsets from the four quadrants cancel each other out. We will return to this point in Section V-B.

When using the OPU in an instrument for nanoscale metrology, the internal gain g of the PDIC is chosen based on the reflectivity of the target. A high gain used with a highly

This article has been accepted for publication in a future issue of this journal, but has not been fully edited. Content may change prior to final publication. Citation information: DOI 10.1109/TIM.2020.3016072, IEEE Transactions on Instrumentation and Measurement

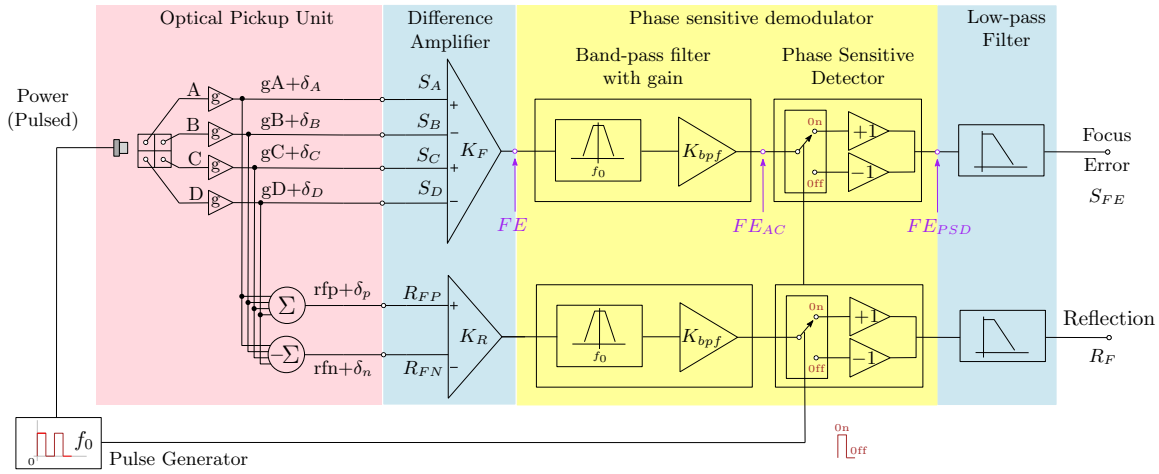

Fig. 5. Proposed measurement scheme using synchronous detection. The laser is driven with a pulsed supply with frequency f_0. The focus error and reflection signals are recovered using a phase sensitive demodulator, consisting of a bandpass filter followed by a phase sensitive detector and a low pass filter.

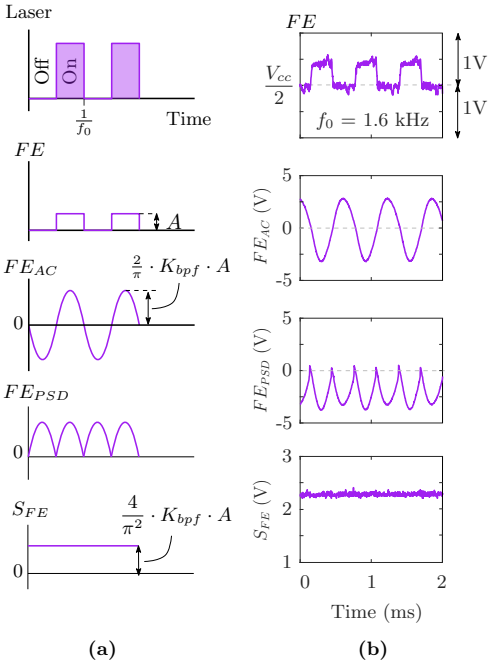

Fig. 6. (a) Typical waveforms at various points of the block diagram presented in Figure 5, showing that the synchronous detection scheme provides an additional gain $\frac{4}{\pi^2} \cdot K_{bpf}$ as compared to the scheme in Figure 3. (b) Measured waveforms from the circuit in Figure 7, using the 405 nm laser pulsed at 1.6 kHz with an amplitude of 2.5V, shining on an aluminium foil. FE is referred with respect to $V_{cc}/2$. Note that FE_{AC} and FE_{PSD} are inverted with respect to those in (a) since our band-pass filter is inverting. However, this is compensated in S_{FE} by the inverting low-pass filter.

reflective target will cause the external difference amplifier to saturate. Imaging a target with poor reflectivity will benefit from the choice of the highest value of g. Note that a constant electrical offset can easily be compensated. However, as we show later in Figure 12, the offsets change significantly with a change in g, making it challenging to using an OPU with targets having a wide range of reflectivities. Our method based on synchronous detection will help overcome this difficulty.

IV. Synchronous Detection

A. Block Diagram and Implementation

The photodetector and electronics in the OPU are designed to have a high bandwidth ($>$ 100MHz) [16] in order to read data from a high-density optical disk spinning at $>$ 1000 rpm. We also find that the laser diodes can be pulsed upto about 20 kHz. Hence the laser diode can be driven by a pulsed supply (with a frequency $f_0 <$ 20kHz) and the component of focus error and reflection at f_0 can be detected synchronously. DC offsets from the OPU will be filtered out. Figure 5 presents an overview of our synchronous detection method. An additional *Phase sensitive demodulator* block, shown in yellow, is included when compared to the scheme presented in Figure 3. This block consists of a band-pass filter (with center frequency f_0 and gain K_{bpf} at f_0) and a switching-type phase sensitive detector (PSD). Figure 6(a) shows the typical waveforms at different points in the block diagram for the focus error. Similar waveforms will be observed for reflection too. The amplitude of the pulsed laser supply is chosen to be identical to that used in the DC measurement technique (Figure 3). The output of the difference amplifier, denoted FE, is a square wave with amplitude A, in phase with the pulsed supply. The band-pass filter extracts the fundamental sinusoidal component of FE, denoted as FE_{AC}, since it has a center frequency matched with the pulse frequency f_0. The PSD multiplies FE_{AC} with a gain $-1/+1$ in phase with the laser being *Off*/*On* to generate FE_{PSD}. Finally, S_{FE} is obtained at output of the low-pass filter which extracts the average value of FE_{PSD}. Compared to the scheme presented in Figure 3, the synchronous detection method described here provides an effective additional gain of $\frac{4}{\pi^2} \cdot K_{bpf}$.

Our implementation of the synchronous detection method is shown in Figure 7. The difference amplifier and low-pass filter are similar to those in Figure 4. All op-amps are implemented using the LM324 integrated circuit. The band-pass filter has a second-order response with center frequency given by

$$f_0 = \frac{1}{2\pi} \cdot \sqrt{\frac{2}{R_{13}R_{14}C_1C_2}} \tag{4}$$

This article has been accepted for publication in a future issue of this journal, but has not been fully edited. Content may change prior to final publication. Citation information: DOI 10.1109/TIM.2020.3016072, IEEE Transactions on Instrumentation and Measurement

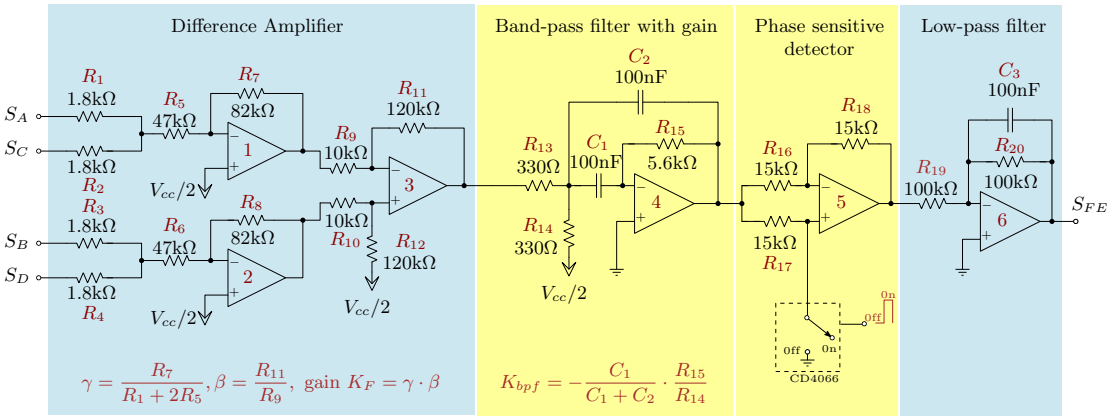

Fig. 7. Circuit diagram for the synchronous detection method. Signals upto the input of the band-pass filter are referred with respect to $V_{cc}/2$. The band-pass filter is designed to operate at 1.6 kHz with a gain $K_{bpf} = -8.5$. Note that both the filters are inverting.

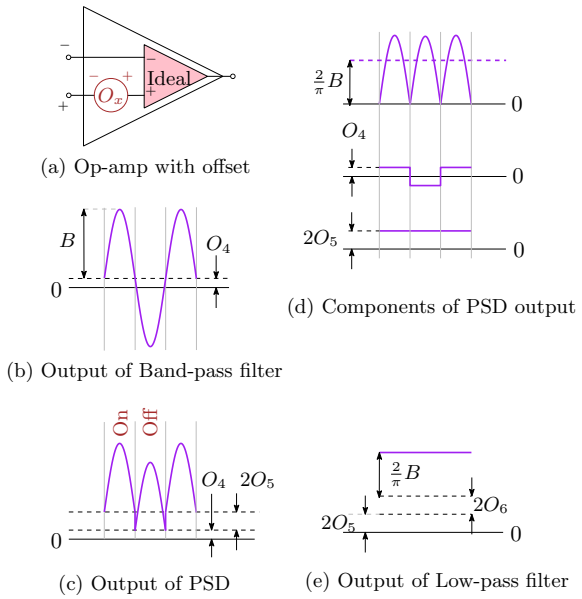

(a) Op-amp with offset

(b) Output of Band-pass filter

(c) Output of PSD

(d) Components of PSD output

(e) Output of Low-pass filter

Fig. 8. Offsets in the synchronous detection method. (a) Model for op-amp with input-referred offset O_x. (b,c) Typical outputs at the band-pass filter and PSD respectively. (d) Components of PSD output, which when filtered give the output (e) at the low-pass filter. Note that all offsets are drawn exaggerated.

and gain (at f_0),

$$K_{bpf} = -\frac{C_1}{C_1 + C_2} \cdot \frac{R_{15}}{R_{14}}. \tag{5}$$

The resistors and capacitors are selected so that f_0 is 1.6 kHz with $K_{bpf} = -8.5$. The PSD uses the CD4066 CMOS switch to toggle the gain of the amplifier built using op-amp 5, based on the pulse driving the laser diode. When the switch is closed (laser *Off*), the PSD behaves likes an inverting amplifier with gain $-R_{18}/R_{16}$ = -1 for the values selected. When the switch is open (laser *On*), the PSD is a superposition of an inverting and non-inverting configuration with net gain +1.

B. Analysis of offsets

As discussed in Section III, offsets in the output arise from the OPU and external electronics. The electrical offsets arise due to mismatch in bias currents inside the integrated circuits, and are hence predominantly DC in nature. While choosing resistors for Figure 7, we ensure that matched resistors have identical values, even if they differ slightly from their nominal indicated values. Hence, we can estimate the total electrical offset by only including the offsets from the op-amps, each modeled as an additional input O_x at the non-inverting terminal, shown in Figure 8. Detailed calculations are available in Appendix A. The band-pass filter removes any DC offset at its input, but includes O_4 (corresponding to op-amp 4) at its output. The PSD output includes an ideal rectified sine-wave, a square wave with amplitude O_4 and a DC offset $2O_5$. The low-pass filter eliminates the square wave component (which has a zero mean), but includes an additional output offset of $2O_6$. Thus, the total electrical offset using synchronous detection is $2O_5 + 2O_6$. The LM324 has a typical input-referred offset of 5mV [20]. Hence, the output offset will typically be within 20 mV. Note that this offset is independent of the internal OPU gain g and external gains K_F and K_{bpf}.

V. Results and Discussion

A. Hardware Setup and Verification

Our setup (Figure. 9) has been designed keeping in mind future extensions for laser scanning microscopy applications. The hardware consists of two aluminium plates: a top plate and a bottom plate. The height of the top plate with respect to the bottom plate can be adjusted manually in a coarse fashion. The OPU is fixed within a 3D printed holder (based on the design available [21], printed on an Ultimaker 2+ printer) and attached to the bottom of the top plate, so that the laser points down. The electronics required to drive the laser diode, and read the analog signals from the OPU are housed in two PCBs, above the top plate. We can control each of the three laser diodes (405 nm, 650 nm and 780 nm) independently, both in the continuous DC mode and pulsed mode. The electronics allows us to switch between the DC and synchronous detection methods. The sample is placed on top of the fixed blue plastic block; this block can be replaced with an XY stage for scanning microscopy. The entire setup is placed on a heavy aluminium slab, kept on a sponge to eliminate vibration. The

This article has been accepted for publication in a future issue of this journal, but has not been fully edited. Content may change prior to final publication. Citation information: DOI 10.1109/TIM.2020.3016072, IEEE Transactions on Instrumentation and Measurement

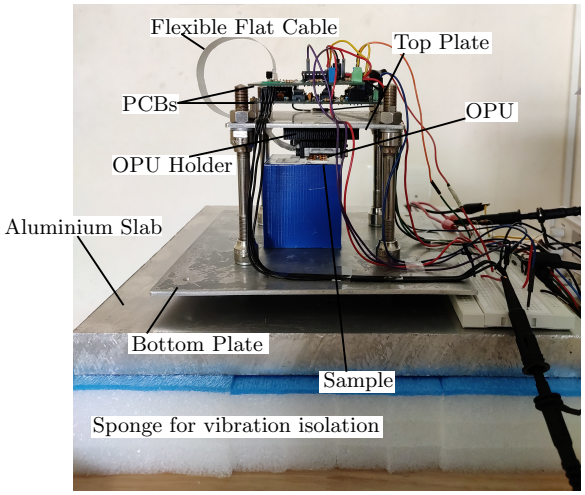

Fig. 9. Hardware setup to measure focus error and reflection. The OPU is fixed with its laser pointing downward. Coarse adjustment of the distance between objective and target is performed manually using four screws. Fine adjustment is performed using the circuit shown in the inset of Figure 10.

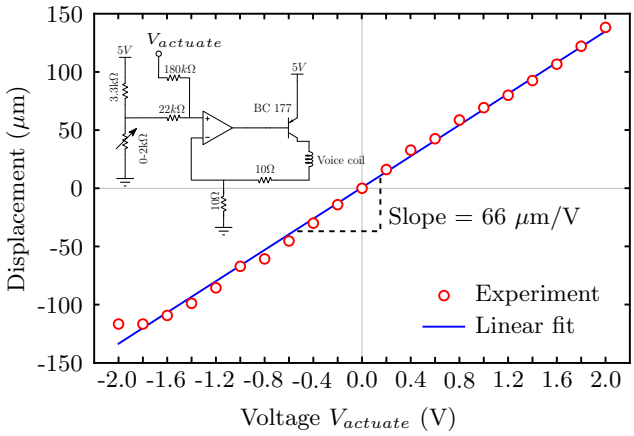

Fig. 10. Sensitivity of the voice coil measured using a non-contact optical profilometer (Nanomap 1000WL, AEP Technology, USA). The potentiometer is adjusted so that 100 mA of current flows through the voice coil when $V_{actuate} = 0$V. Inset shows the drive circuit for the voice coil actuator.

setup is covered by a box (not shown in picture) to reduce the effects of external light and atmospheric vibration.

In order to measure the focus error and reflection as functions of defocus distance, fine adjustment of the distance between the objective lens and the target is achieved using the circuit shown in the inset of Figure 10. First, keeping $V_{actuate}$ = 0V, the potentiometer is adjusted so that the target lies at the focal point of the objective lens, with about 100 mA of current flowing through the voice coil. The focal point is found most easily by using the synchronous method and looking at FE_{PSD} on an oscilloscope; around focus, this signal changes phase by 180^o. Next, $V_{actuate}$ is varied from -2V to +2V as a periodic ramp (with a ramp rate of 4V/s) using a signal generator (Tektronix AFG1022). S_{FE} and R_F are captured as functions of time using a digital storage oscilloscope (Tektronix TDS2014C). They are converted to functions of displacement using the sensitivity (μm/V) of the voice coil.

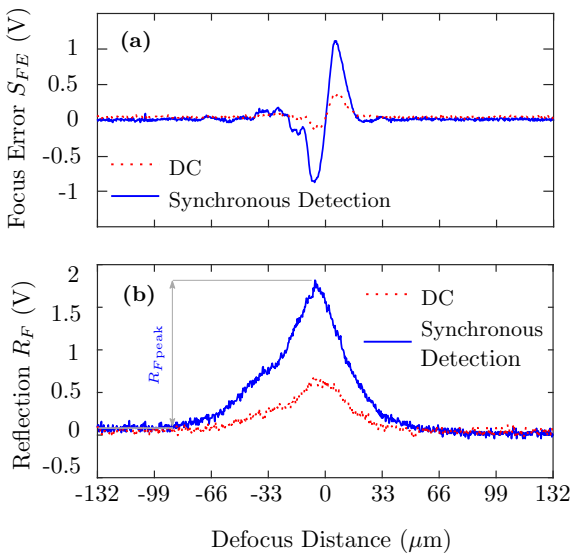

Fig. 11. Focus Error and Reflection obtained from the DC and synchronous detection methods for an aluminium foil (PDIC Gain g = 2). The peak reflection in the synchronous method has also been indicated and will be refered to in Section V-B. Note that the result from the DC method has been inverted and a shift of $V_{cc}/2$ has been removed, owing to the slight differences in the implementation of Figure 4 and Figure 7.

The voice coil has a dynamic range of around 1 mm [8]. Figure 10 shows the result of a separate experiment to measure the response of the voice coil actuator. Here, the OPU is placed (along with its holder) with its laser pointing upward, on the stage of a non-contact optical profilometer(Nanomap 1000WL, AEP Technology, USA). The potentiometer is adjusted so that the voltage at the non-inverting terminal of the op-amp is 1V when $V_{actuate}$ = 0V. $V_{actuate}$ is varied in steps from -2V to +2V. The optical profilometer provides a 0.1 μm resolution over this range of displacement. As shown, a sensitivity of 66 μm/V is obtained for the voice coil actuator. From the error between the linear fit and experimental data, we estimate the positional accuracy of the voice coil actuator to be within about 5 μm.

We verify the proper working of our setup by measuring the focus error and reflection from a piece of aluminium foil using the DC and synchronous detection methods (Figure 11). The PDIC gain g is set at 2 since the sample is highly reflective. While plotting the result of the DC method, we have subtracted $V_{cc}/2$, in order to account for the fact that the PHR-803T references all outputs with respect to $V_{cc}/2$. Additionally, we have multiplied the result by -1 to account for the additional inversion provided by the circuit implementation (Figure 4) for the DC method as compared to the synchronous detection method (Figure 7). Note that the relative magnitude of the signals is consistent with our estimate of the synchronous detection scheme providing an additional gain of $\frac{4}{\pi^2} \cdot K_{bpf} = \frac{4}{\pi^2} \times 8.5 \approx 3.4$.

B. Reduction of offsets in Focus Error

As discussed in Section II-B, the focus error is expected to become zero for large defocus distance. However electrical offsets can cause a shift away from zero. We fabricate a dark

This article has been accepted for publication in a future issue of this journal, but has not been fully edited. Content may change prior to final publication. Citation information: DOI 10.1109/TIM.2020.3016072, IEEE Transactions on Instrumentation and Measurement

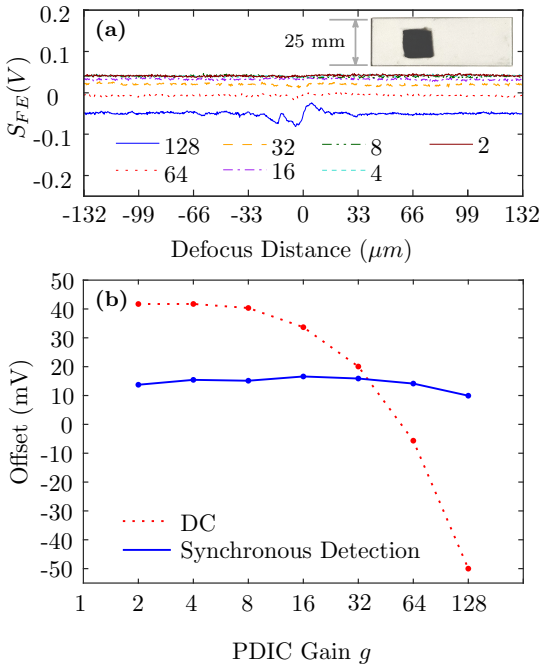

Fig. 12. (a) Focus error signal S_{FE} obtained from a glass slide coated with soot, using the DC method, with different PDIC gains $g \in \{2, 4, 8, 16, 32, 64, 128\}$. Inset shows the soot glass slide coated with soot. (b) Offsets in S_{FE} using the DC and synchronous methods. Note that offset in the latter method is significantly smaller and is relatively invariant of g.

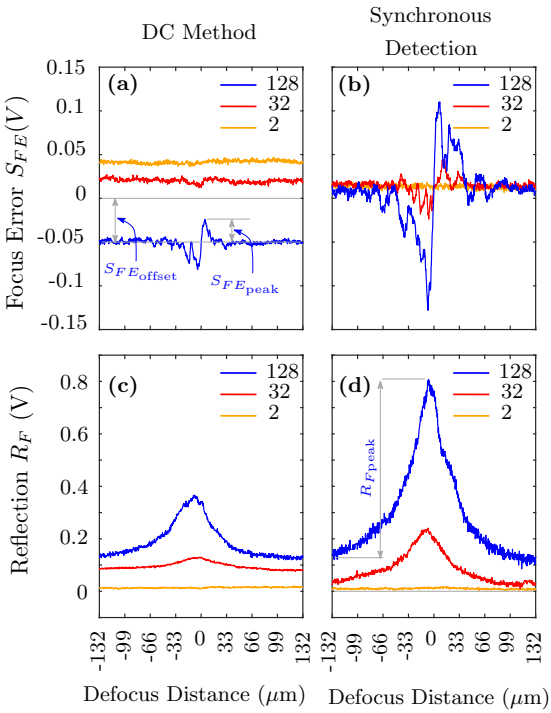

Fig. 13. Focus error S_{FE} and Reflection obtained from a glass slide coated with soot for PDIC gain $g \in \{2, 32, 128\}$ using the (a, c) DC method and (b, d) synchronous detection method. Note that the peak in the focus error measured using the DC method is swamped by the offset.

sample by holding a glass slide above the flame of a paraffin candle for about a minute. This process is similar to the one described in [22], wherein Scanning Electron Microscopy (SEM) reveals carbon particles to have a typical diameter of 30 - 40 nm. These particles are smaller than the resolution of the OPU, and the soot layer can be considered as a uniform, dark target for our measurement. Figure 12(a) shows the focus error obtained from the glass slide coated with a layer of soot, using the standard DC method (inverted and shifted by $V_{cc}/2$, as in Figure 11). Note that the offset of the focus error from zero, at large defocus distance, changes significantly as a function of PDIC gain g. Figure 12(b) compares these offsets obtained using the DC method with those measured for the synchronous detection method. Clearly, the latter is significantly lower than the former. Further, it is almost constant with a change in PDIC gain, and lies within the expected bound of $2O_5 + 2O_6 = 20$ mV, as expected from our earlier analysis (Section IV-B).

Soot is a very poorly reflecting target. Even at the highest PDIC gain ($g = 128$), the amplitude of the focus error is completely swamped by the offset of the DC method. No additional amplification can change the relative magnitudes of the amplitude and offset. On the other hand, the focus error obtained using the synchronous detection method has a small offset ($\sim$ 10-15 mV) as compared to its amplitude ($\sim$ 100 mV), as shown in Figure 13 (a, b). Further, since this offset is almost constant with respect to PDIC gain g, it can easily be subtracted out while being used in a focus control loop.

Figure 13 (c, d) show the reflection R_F obtained using the DC and synchronous detection methods. Unlike in the case of focus error, the synchronous detection method does not reduce the offset at large defocus distance. This is because optical offsets, caused by internal reflections in the OPU, also contribute to the measured offset in R_F, as discussed in Section III.

The aluminium foil has a reflectivity in the range 86% to 88% [23]. Comparing $R_{F\text{peak}}$ in the DC and synchronous detection methods (Figures 11(b), 13(d)), and including the different values of g used, we estimate the reflectivity of the dark sample to be $\sim$ 0.5%. Thus, our measurements indicate that the synchronous detection method has a dynamic range of at least $\sim 170\times$.

In the synchronous method for the dark sample (Figure 13(b)), the peak of the S_{FE} is almost $10\times$ the offset. When used in the control loop indicated in Figure 1, this should ensure that the measured reflection is close to the true peak reflection. To achieve a similar robust measurement in DC method, the peak of S_{FE} should be atleast $10\times$ the offset $\equiv$ 0.5V, i.e. the reflectivity of the sample should be at least $20\times$ the reflectivity of our dark sample. Thus, we estimate that the synchronous detection method can achieve an improvement of $20\times$ in the minimum reflectivity that can be robustly, as compared to the DC method.

As a closing remark, it is important to note that the maximum offset in S_{FE} in the synchronous method ($2O_5 + 2O_6$) can be reduced by using low-offset opamps; however the maximum offset in the DC method can be as large as $K_F \times (|\delta_A| + |\delta_B| + |\delta_C| + |\delta_D|)$ even in the absence of opamp offsets. Further, increasing K_{bpf} in the synchronous method amplifies the peak focus error and reflection, without adding any offset.

VI. Conclusion

An OPU is a low cost, portable and easily available instrument that can be used for many optical sensing applications. We have presented a synchronous detection based method, wherein a pulsed laser diode is used to reduce the offsets in focus error. We have shown analytically, and demonstrated experimentally, that the offset in our method is (i) significantly lower in magnitude and (ii) relatively invariant of the photodetector gain selected, than in the typical DC method (which uses a continuously powered laser diode). This work should facilitate measurement of reflectivity of poorly reflecting samples, wherein the DC measurement method may result in a focus error signal whose amplitude is swamped by an offset. We believe that our method can hence increase the dynamic range of reflectivities that an instrument made using an OPU can measure. Further, the setup in Figure 9 be extended for low cost imaging applications, where the OPU can be scanned over the substrate and change in reflectivities could be detected. The cost of such a system could be as low as USD 1500 when a low-cost XY stage (such as [24]) is used to move the sample. Finally, note that the advantages of the synchronous method are achieved as a trade-off against the bandwidth available in the DC method.

Appendix A
Calculation of Offsets

Let O_4, O_5 and O_6 be the input-referred offsets of opamps 4, 5, 6 in figure 7. Let V_{in} and V_{out} represent the input and output of each functional block. Further, we set $R_{13} = R_{14}$, $R_{16} = R_{18}$ and $R_{19} = R_{20}$. Then the band-pass filter follows

$$V_{out}(s) = O_4(s) + (2O_4(s) - V_{in}(s))\times \left[\frac{sR_{15}C_1}{2 + sR_{14}(C_1 + C_2) + s^2R_{14}R_{15}C_1C_2}\right] \quad \text{(A.1)}$$

Hence any DC offset at the input V_{in} of the bandpass filter is filtered out. The output has a DC offset equal to the input offset O_4. In the phase sensitive detector, the output V_{out} due to the input V_{in} and offset O_5 is given by

$$V_{out} = \begin{cases} -\frac{R_{18}}{R_{16}}V_{in} + \left(1 + \frac{R_{18}}{R_{16}}\right)O_5, \text{ switch closed} & \text{(A.2)} \\ V_{in} + \left(1 + \frac{R_{18}}{R_{16}}\right)O_5, \text{ switch open} & \text{(A.3)} \end{cases}$$

Hence the total offset at the output is $2O_5$ whether the switch is closed or open. The low pass filter follows

$$V_{out}(s) = O_6(s) + \frac{O_6(s) - V_{in}(s)}{1 + sR_{20}C_3} \quad \text{(A.4)}$$

with an output DC offset of $2O_6$.

Thus, in the synchronous detection method, the offsets created by the OPU and op-amps 1, 2 and 3 are removed by the band pass filter. The offset provided by the op-amp 4 is removed by the phase sensitive detector (PSD). Hence, the total offset in synchronous detection method is only due to op-amps 5 and 6, giving a total offset

$$V_{offset} = 2O_5 + 2O_6. \quad \text{(A.5)}$$

Acknowledgment

The authors acknowledge the Central Instrumentation Facility (CIF) of Indian Institute of Technology, Palakkad. The authors also thank Dr. Revathy Padmanabhan and Dr. Sreenath Vijayakumar, IIT Palakkad for useful discussions.

References

[1] *White Paper: Blu-ray Disc Format*, 2010.
[2] A. H. Chaghajerdi, "Sensing and control in optical drives how to read data from a clear disc," *IEEE Control Systems*, vol. 28, no. 3, 2008.
[3] E.-T. Hwu, H. Illers, L. Jusko, and H.-U. Danzebrink, "A hybrid scanning probe microscope (SPM) module based on a DVD optical head," *Meas. Sci Technol.*, vol. 20, no. 8, p. 084005, jun 2009.
[4] Y.-C. Liu, K.-C. Fan, C.-L. Chu, C. A. Werner, and G. Jäger, "Development of an optical accelerometer for low-frequency vibration using the voice coil on a DVD pickup head," *Meas. Sci. Tech.*, vol. 19, no. 8, p. 084012, Jul 2008.
[5] C.-L. Chu, C.-H. Lin, and K.-C. Fan, "Two-dimensional optical accelerometer based on commercial DVD pick-up head," *Meas. Sci. Tech.*, vol. 18, no. 1, pp. 265–274, Dec 2006.
[6] C.-L. Chu and C.-H. Lin, "Development of an optical accelerometer with a DVD pick-up head," *Meas. Sci. Tech.*, vol. 16, no. 12, pp. 2498–2502, Nov 2005.
[7] T. Carlson, "High speed atomic force microscope design using dvd optics," Ph.D. dissertation, Virginia Commonwealth University, 2014.
[8] E. E.-T. Hwu and A. Boisen, "Hacking CD/DVD/Blu-ray for Biosensing," *ACS Sensors*, vol. 3, no. 7, pp. 1222–1232, 2018.
[9] Bañuls, María-José and González-Pedro, María-Victoria and Puchades, Rosa and Maquieira, Ángel, "Influenza A virus infection diagnosis based on DVD reader technology," *Anal. Methods*, vol. 4, no. 10, pp. 3133–3139, 2012.
[10] L. I. Segerink, M. J. Koster, A. J. Sprenkels, and A. van den Berg, "A low-cost 2D fluorescence detection system for μm sized beads on-chip," *Lab on a Chip*, vol. 12, no. 10, pp. 1780–1783, 2012.
[11] E.-T. Hwu, S.-K. Hung, C.-W. Yang, I.-S. Hwang, and K.-Y. Huang, "Simultaneous detection of translational and angular displacements of micromachined elements," *Appl. Phys. Lett.*, vol. 91, no. 22, p. 221908, 2007.
[12] E.-T. Hwu, K.-Y. Huang, S.-K. Hung, and I.-S. Hwang, "Measurement of Cantilever Displacement Using a Compact Disk/Digital Versatile Disk Pickup Head," *Japanese J. Appl. Phys.*, vol. 45, no. 3S, p. 2368, 2006.
[13] Kuang-Yuh Huang, En-Te Hwu, Hsin-Yi Chow, and Shao-Kan Hung, "Development of an optical pickup system for measuring the displacement of the micro cantilever in scanning probe microscope," in *IEEE International Conference on Mechatronics, 2005. ICM '05.*, July 2005, pp. 695–698.
[14] F. Bosco, E. T. Hwu, S. Keller, A. Greve, and A. Boisen, "Self-aligned cantilever positioning for on-substrate measurements using DVD pickup head," *Microelectronic Engineering*, vol. 87, no. 5, pp. 708 – 711, 2010.
[15] L. Cabriales, M. Hautefeuille, G. Fernández, V. Velázquez, M. Grether and E. López-Moreno, "Rapid fabrication of on-demand high-resolution optical masks with a CD-DVD pickup unit," *Appl. Opt.*, vol. 53, no. 9, pp. 1802–1807, Mar 2014.
[16] *Melexis MLX75012 Datasheet*, 2007.
[17] J. Chou, L. Parameswaran, B. Kimball, and M. Rothschild, "Electrically switchable diffractive waveplates with metasurface aligned liquid crystals," *Opt. Express*, vol. 24, no. 21, pp. 24 265–24 273, Oct 2016.
[18] S. McMillan, "DVD Optical System Design," University of Colorado Boulder.
[19] B. Hnilička, A. Voda, and H.-J. Schröder, "Modelling the characteristics of a photodetector in a DVD player," *Sens. Actuator A Phys.*, vol. 120, no. 2, pp. 494 – 506, 2005.
[20] *LM324 Datasheet*, Texas Instruments.
[21] "Diyouware Twinteeth." http://www.diyouware.com/twth_getit
[22] X. Deng, L. Mammen, H.-J. Butt, and D. Vollmer, "Candle soot as a template for a transparent robust superamphiphobic coating," *Science*, vol. 335, no. 6064, pp. 67–70, 2012.
[23] V. Pozzobon, W. Levasseur, K.-V. Do, B. Palpant, and P. Perré, "Household aluminum foil matte and bright side reflectivity measurements: Application to a photobioreactor light concentrator design," *Biotechnology Reports*, vol. 25, p. e00399, 2020.
[24] R. A. A. Campbell, R. W. Eifert, and G. C. Turner, "Openstage: A low-cost motorized microscope stage with sub-micron positioning accuracy," *PLOS ONE*, vol. 9, no. 2, pp. 1–18, 02 2014.